Proc. Natl. Acad. Sci. USA
Vol. 96, pp. 2880–2884, March 1999
Genetics

GLI3 mutations in human disorders mimic *Drosophila* Cubitus interruptus protein functions and localization

SANG HOON SHIN*, PRIIT KOGERMAN†, ERIKA LINDSTRÖM†, RUNE TOFTGÁRD†, AND LESLIE G. BIESECKER*‡

*National Institutes of Health, National Human Genome Research Institute, Genetic Disease Research Branch, Bethesda, MD 20892; and †Karolinska Institute, Department of Bioscience, Huddinge, Sweden

Communicated by Francis S. Collins, National Institutes of Health, Bethesda, MD, December 31, 1998 (received for review December 8, 1998)

ABSTRACT **Truncation mutations of the *GLI3* zinc finger transcription factor can cause Greig cephalopolysyndactyly syndrome (GCPS), Pallister–Hall syndrome (PHS), and postaxial polydactyly type A (PAP-A). GLI3 is homologous to *Drosophila* Cubitus interruptus (Ci), which regulates the *patched* (*ptc*), *gooseberry* (*gsb*), and *decapentaplegic* (*dpp*) genes. Ci is sequestered in the cytoplasm and is subject to posttranslational processing whereby the full-length transcriptional activator form (Ci^{155}) can be cleaved to a repressor form (Ci^{75}). Under hedgehog signaling, the Ci^{155} form translocates to the nucleus whereas in the absence of hedgehog, the Ci^{75} form translocates to the nucleus. Based on the correlation of GLI3 truncation mutations and the human phenotypes, we hypothesized that GLI3 shows transcriptional activation or repression activity and subcellular localization similar to Ci. Here we show that full-length GLI3 localizes to the cytoplasm and activates *PTCH1* expression, which is similar to full-length Ci^{155}. PHS mutant protein (GLI3-PHS) localizes to the nucleus and represses GLI3-activated *PTCH1* expression, which is similar to Ci^{75}. The GCPS mutant protein has no effect on GLI3-activated *PTCH1* transcription, consistent with the role of haploinsufficiency in this disorder. The PAP-A mutant protein (GLI3-PAP-A) showed less specific subcellular localization but still inhibited GLI3-activated *PTCH1* transcription, suggesting it may be a weaker allele than the GLI3-PHS mutation. These data show that *GLI3* mutations in humans mimic functional effects of the *Drosophila ci* gene and correlate with the distinct effects of these mutations on human development.**

The *GLI3* gene originally was cloned by homology to *GLI* and subsequently was shown to be interrupted by translocations in patients with the Greig cephalopolysyndactyly syndrome (GCPS) (1). Subsequently, it was demonstrated that mutations in *GLI3* can cause the Pallister–Hall syndrome (PHS) (2) and postaxial polydactyly type A (PAP-A) (3). These findings raised the question of how distinct human developmental disorders (GCPS and PHS) and isolated anomalies (PAP-A) can be caused by mutations in a single gene. The GCPS mutations that have been described (truncations, deletions, point mutations, and translocations) support the previous assertions that haploinsufficiency of *GLI3* causes GCPS whereas frameshift mutations alone are known to cause PHS and PAP-A. Because all three disorders can be caused by frameshift mutations, we chose to investigate the potential correlation of the position of truncation mutations and the effect of those mutations on GLI3 localization and function as a possible explanation for the distinct phenotypes (4). The model is based on the homology of GLI3 to the Drosophila *cubitus interruptus* gene product, Ci (5). In *Drosophila*, Ci exists as a 155-kDa full-length form (Ci^{155}) that has been shown to be anchored indirectly to the microtubular apparatus in the cytoplasm in a complex with the *costal2, fused,* and *suppressor of fused* [*su(fu)*] gene products (6–8). The Ci protein can undergo proteolytic processing and be released as a 75-kDa truncated product (Ci^{75}) that represses downstream genes (*ptc, gsb,* and *dpp*), or it may be released in the Ci^{155} form and activate transcription of these genes (6, 9). The balance of activator and repressor forms is regulated by hedgehog signaling, mediated through patched/smoothened transduction (7). We hypothesized that the human truncation mutations in *GLI3* cause distinct disorders of human development because of the presence or absence of key functional domains and that these proteins activate or repress downstream genes in a manner predicted by the dual forms of *Drosophila* Ci. Phenotypic analyses show that although PHS and GCPS share some features (e.g., postaxial polydactyly), they have nonoverlapping manifestations and are distinct syndromes (10, 11). PAP-A is a nonsyndromic form of autosomal-dominant postaxial polydactyly (3) and could be considered a mild form of either GCPS or PHS. GCPS and PHS cannot be placed on a single phenotypic continuum of severity, implying that there are distinct pathogenetic mechanisms producing the different anomalies in these two disorders. On the basis of these data, we hypothesized that the truncation mutations caused distinct developmental anomalies because of the inclusion or loss of these functional domains (4). We chose to model these mutations by comparing the effects of truncated GLI3 proteins: GCPS is modeled after the truncation mutation that deletes the zinc fingers and domains 3–7 (12), PHS deletes domains 3–7 (2), and PAP-A deletes domains 4–7 (3) (see Fig. 1*A*).

MATERIALS AND METHODS

Construction of *GLI3* Truncation Mutants. A series of mutants that generate C-terminal truncated proteins of GLI3 was constructed by PCR amplification and subcloning of full-length human *GLI3* cDNA pGli3bs-2 (5). Primers GFP5′ (5′-TAGCTGACGAGCTCAGAAGACATCATGGAGG-3′) and GFPtrunc3′ (5′-GATCGCTAGAGCTCAAC-CAAGGGCTCCCTGAGT-3′) were used to amplify *GLI3* cDNA from the initiator codon to codon 675. This fragment was cloned into the *Sac*I site of pEGFP-C2 (CLONTECH) to generate plasmid EGLI3-PHS. *GLI3* cDNA from the initiator codon to codon 423 was cloned by excising a *Sac*I and *Pst*I fragment from EGLI3-PHS and ligating it into the *Sac*I and *Pst*I sites of pEGFP-C2 to generate plasmid EGLI3-GCPS. Primers GFP5′ and R764ter (5′-GCGCGCGTCGACCTAT-TGCAAAGCAAGGGCTGTGGT-3′) were used to generate a *Sac*I and *Sal*I fragment of *GLI3* cDNA from the initiator codon to codon 764, which was cloned into pEGFP-C2 to

The publication costs of this article were defrayed in part by page charge payment. This article must therefore be hereby marked "*advertisement*" in accordance with 18 U.S.C. §1734 solely to indicate this fact.

PNAS is available online at www.pnas.org.

Abbreviations: PHS, Pallister–Hall syndrome; GCPS, Greig cephalopolysyndactyly syndrome; PAP-A, postaxial polydactyly type A.

‡To whom reprint requests should be addressed at: National Institutes of Health, National Human Genome Research Institute, Genetic Disease Research Branch, Building 49, Room 4A80, Bethesda, MD 20892-4472. e-mail: leslieb@helix.nih.gov.

generate plasmid EGLI3-PAP-A. A 4.8-kb *Eco*RI fragment of pGli3bs-2 was cloned into the *Eco*RI site of EGLI3-PHS construct to generate EGLI3-FL, full-length GLI3. Correct insert orientation was determined by digestion with *Sac*I and *Sal*I to generate a 4.9-kb *GLI3* fragment and a 4.6-kb pEGFP backbone vector. To generate amino-terminal enterokinase-tagged constructs, EGLI3-GCPS, EGLI3-PAP-A, and EGLI3-FL were digested by *Sac*I, blunted with T4 DNA polymerase, digested with *Sal*I, and ligated into *Eco*RV and *Xho*I-digested pcDNA3.1HisC vector (Invitrogen) to generate GLI3-GCPS, GLI3-PAP-A, and GLI3-FL, respectively. EGLI3-PHS was digested with *Sac*I, blunted with T4 DNA polymerase, and ligated into pcDNA3.1HisC, which was digested with *Apa*I, blunted with T4 DNA polymerase, and digested again with *Eco*RV to generate GLI3-PHS. All PCR-derived products were confirmed by sequencing.

Western Blotting. Lysates were prepared from cells 24 hr after transfection. Aliquots of lysates were separated on 4–15% SDS-polyacrylamide gel, transferred to poly(vinylidene difluoride) membrane (Millipore), and probed with a 1:5,000 dilution of Anti-Xpress antibody (Invitrogen). Immunodetection with sheep anti-mouse horseradish peroxidase conjugate and enhanced chemiluminescence (Amersham) was performed according to the manufacturer's instructions.

Immunofluorescence. HeLa cells (ATCC CCL2) were cultured according to the distributor and seeded onto glass coverslips in six-well plates 12 hr before the calcium phosphate transfection (Stratagene) with plasmid DNAs, using the manufacturer's instructions. After 24 hr, cells were fixed with 1% paraformaldehyde for 20 min, washed with PBS twice, and permeated with 0.05% Triton X-100 for 10 min. The cells were blocked with 5% BSA in PBS for 30 min, rinsed in 1% BSA in PBS, immunostained with 1:400 dilution of Anti-Xpress antibody (Invitrogen), washed with 1% BSA five times, incubated with 1:400 secondary antibody coupled to tetramethylrhodamine B isothiocyanate (Sigma), and washed with 1% BSA once. Fluorescence microscopy was performed by using a Zeiss Axiophot microscope, and images were captured with a Photometrics CH250 liquid-cooled charge-coupled device camera. Images were processed with the IP LAB (Scanalytics, Fairfax, VA) software package on a Macintosh 8100/110 computer. At least 100 transfected cells were counted for each construct. Cells were scored as nuclear, cytoplasmic, or mixed (nuclear and cytoplasmic) signal pattern. These experiments were repeated in 293 cells lines and gave similar results (data not shown).

GLI3 Transcriptional Activity. The *PTCH1* genomic region was cloned as described previously (13). A 4.3-kb fragment of the 5′ regulatory region was subcloned into the pGL3-Basic vector (Promega) upstream of the firefly luciferase reporter gene. It was demonstrated that this construct can mediate activation of the reporter gene in different cell lines in response to expression of *GLI1* and *SHH* cDNA (P.K. and R.T., unpublished observations).

Human 293 cells (kidney epithelial cell line) were obtained from American Type Culture Collection and grown in DMEM supplemented with penicillin and streptomycin and 10% fetal bovine serum (GIBCO/BRL). Cells were passaged to 24-well plates the day before experiments, and transfections were carried out with DNA complexed to the Superfect transfection reagent (Qiagen) according to the manufacturer's instructions. Twenty-four hours after transfection, the medium was removed and the cells were lysed in Somalyze lysis buffer (BioOrbit, Turku, Finland). Luciferase activity was determined on a BioOrbit 1250 Luminometer by using BioOrbit Luciferin Substrate and ATP reagents according to the manufacturer's instructions. The results from at least six experiments from two separate transfections were compiled. The results were normalized for transfection efficiency and protein expression by measuring β-galactosidase activity generated from an Rous sarcoma virus–lacZ expression construct that was cotransfected into each well. This activity was measured by using the luminometric GalactoLight Plus assay (Tropix, Bedford, MA) according to the manufacturer's instructions.

Statistical analyses were performed by using Student's *t* test unless data showed evidence of unequal SDs (F test, $p < 0.05$). In these cases, the Mann–Whitney nonparametric test was used. All calculations were performed by using the INSTAT program (GraphPad, San Diego).

RESULTS

Subcellular Localization of GLI3 Proteins. The model predicted that GLI3 proteins would be localized into subcellular compartments similarly to processed and unprocessed Ci. We tested this model first by determining the subcellular localization of various truncated mutants of the GLI3 protein in HeLa cells. A series of *GLI3* expression constructs was made to mimic the frameshift mutations found in GCPS (423 aa), PHS (674 aa), and PAP-A (764 aa) in addition to full-length GLI3 (1596 aa) (Fig. 1*A*). The hypothesis predicted that GLI3-FL would be localized to the cytoplasm as seen in intact Ci^{155}, that a GLI3-PHS protein would localize to the nucleus, as does Ci^{75}, and that GLI3-GCPS protein would show cytoplasmic or nonspecific localization because it is lacking the putative nuclear localization signal in the C-terminal end of the zinc finger domain.

Subcellular localization was performed by using *GLI3* cDNA constructs fused with an amino-terminal enterokinase (EK) epitope. The constructs produced epitope-GLI3 chimeric proteins of the predicted size (Fig. 1*B*). Amino-terminal EGFP-tagged GLI3 proteins yielded similar results (data not shown). Transfection of the GLI3-FL construct showed punctate cytoplasmic fluorescence in 97% of transfected cells ($n = 211$) (Fig. 2*A*). In contrast, the GLI3-PHS protein showed nuclear fluorescence in 86% of transfected cells ($n = 273$) (Fig. 2*C*). The GLI3-GCPS protein showed a mixed pattern with about 1/3 of transfected cells ($n = 139$), each showing nuclear, cytoplasmic, and mixed nuclear and cytoplasmic signals (Fig. 2*B*). The GLI3-PAP-A construct produced a protein that showed inconsistent staining, with most cells showing either a cytoplasmic pattern (49%, $n = 270$) or a nuclear pattern (41%) and fewer (10%) showing a mixed nuclear and cytoplasmic pattern (Fig. 2*D*). The dramatic difference between the GLI3-FL and GLI3-PHS localization data shows that the targeting of normal and truncated GLI3 proteins mimics that of Ci^{155} and Ci^{75}, respectively. These observations are consistent with the proposed model.

GLI3 Transcriptional Regulation of *PTCH1*. To further address the issue of the distinct developmental consequences of various *GLI3* mutations, we next determined the transcriptional activation properties of full-length and truncated forms of GLI3. We hypothesized that full-length and truncated GLI3 proteins can have activator and repressor activities similar to full-length and truncated forms of Ci, respectively. In this model, full-length GLI3 was proposed to activate transcription, similar to Ci^{155} and full-length GLI1 (14). The GLI3-PHS construct was predicted to repress transcriptional activity constitutively, based on the transcriptional repressor effect of processed *Drosophila* Ci^{75}. In addition, the GLI3-GCPS and GLI3-PAP-A proteins have effects that can be predicted from what is known about Ci, although they do not reflect normal functions of Ci. Specifically, we hypothesized that the GLI3-GCPS construct would show no repression or activation, being effectively a null allele, whereas the GLI3-PAP-A construct was predicted to cause weak repression activity because of the lack of a transcription activation domain (4). To test these hypotheses, a 4-kb 5′ promoter region of the human *PTCH1* gene containing several putative GLI-binding sites was coupled to a luciferase reporter and transfected into 293 cells along with GLI3 mutation constructs. The *PTCH1* promoter

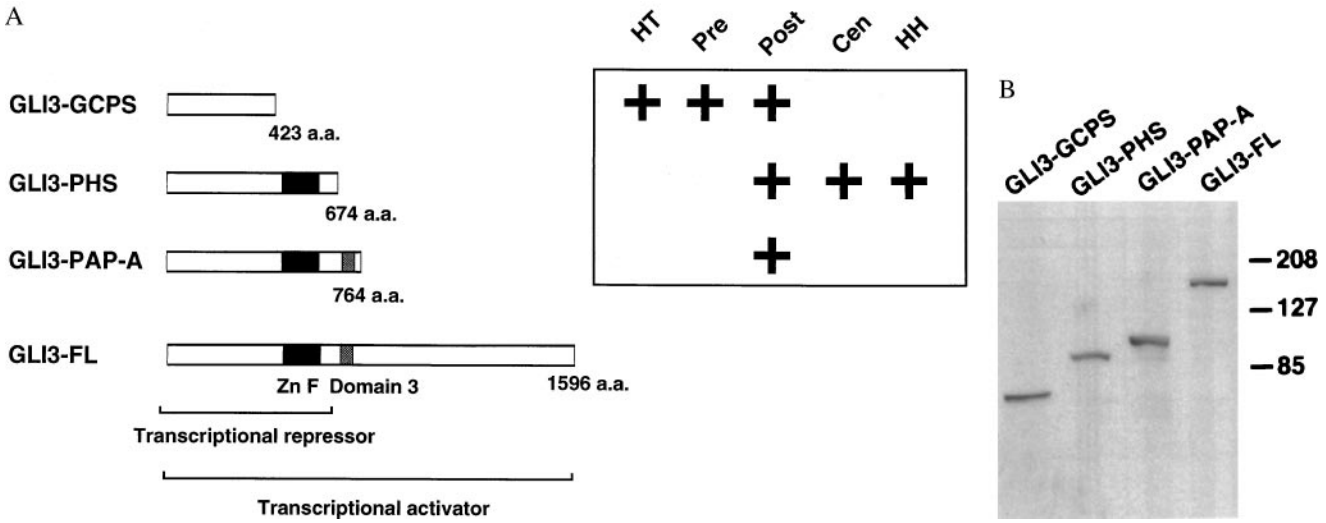

FIG. 1. Construction and expression of mutant and full-length GLI3. (*A*) *GLI3* constructs including full-length (GLI3-FL) and three truncations that model mutations in human developmental malformations including GLI3-GCPS, GLI3-PHS, and GLI3-PAP-A. All constructs include an amino-terminal enterokinase recognition site (anti-Xpress epitope) tag. The zinc finger domain (Zn F) and domain 3 are shown as their presence or absence varies among the human truncation mutations. It has been hypothesized previously that full-length GLI3 is a transcriptional activator and truncated GLI3 (GLI3-PHS) is a transcriptional repressor. The major phenotypic features are shown to the left of the figure. HT, hypertelorism; Pre, preaxial polydactyly; Post, postaxial polydactyly; Cen, central polydactyly; HH, hypothalamic hamartoma. (*B*) Western blot of transfected cell lines with anti-Xpress antibody showing the production of proteins of the predicted sizes from GLI3-GCPS, GLI3-PHS, GLI3-PAP-A, and GLI3-FL constructs. The size of full-length GLI3 was reported previously as 190 kDa (5), similar to the result shown here.

was used for these experiments because *PTCH1* is known to be regulated by GLI3 (15). The GLI3-FL transfection caused a statistically significant activation of *PTCH1* reporter gene activity whereas the GLI3-PHS construct caused a dose-dependent repression of basal *PTCH1* expression as well as inhibition of the transcriptional activation by GLI3-FL (Fig. 3). As predicted, GLI3-GCPS showed no effect on *PTCH1* expression, attributable to its absence of DNA-binding domains and defective subcellular targeting (data not shown). The GLI3-PAP-A construct showed no repression of basal transcriptional, but it did repress *PTCH1* transcription activation induced by GLI3-FL (Fig. 3). Similar data were obtained using full-length GLI1 as the activator (data not shown).

DISCUSSION

The activation of the *PTCH1* promoter by GLI3-FL is the first demonstration of transcription activation by GLI3 and is

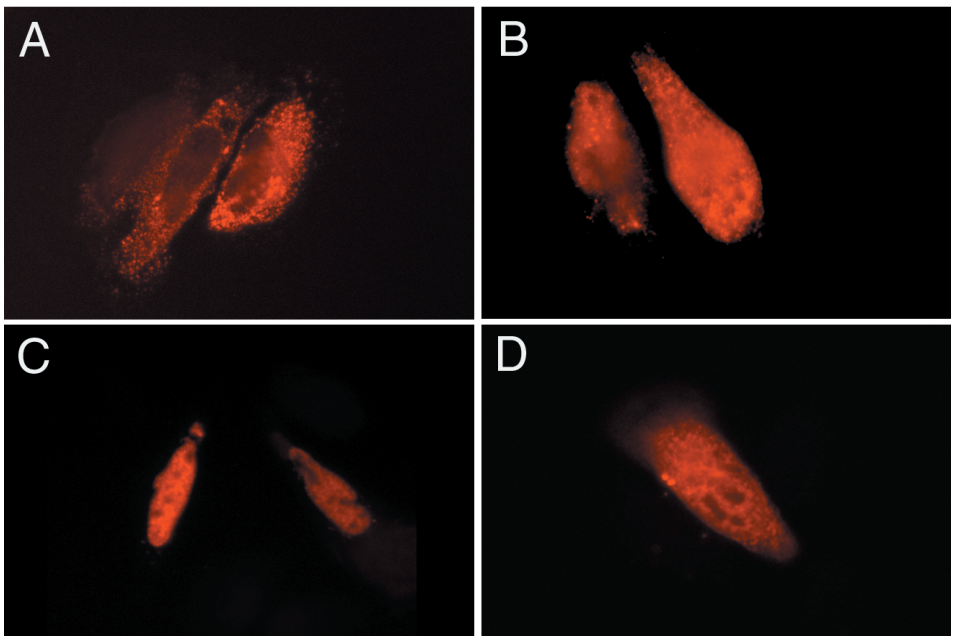

FIG. 2. GLI3 subcellular localization. (*A*) The full-length, wild-type GLI3-FL transfection showed cytoplasmic staining consistent with the known subcellular localization of the *Drosophila* Ci^{155} protein. (*B*) Fluorescence microscopy image of GLI3-GCPS protein showing nonspecific and variable cytoplasmic and nuclear immunofluorescence signal. This staining pattern is consistent with a model that predicts aberrant targeting of GLI3-GCPS protein resulting from absence of both the cytoplasmic anchor and the nuclear localization signal. (*C*) The GLI3-PHS protein gave a strong and consistent nuclear staining that mimics the effect of the *Drosophila* Ci^{75} processed protein, which is targeted to the nucleus. (*D*) The GLI3-PAP-A construct gave a result similar to the GLI3-GCPS construct, with a mix of cytoplasmic and nuclear staining. The GLI3-PAP-A pattern is attributed to inefficient cytoplasmic anchoring because of partial function of the cytoplasmic anchor. The *Results* section includes data on cell counts for each subcellular localization pattern. Each transfection was scored in at least 139 cells.

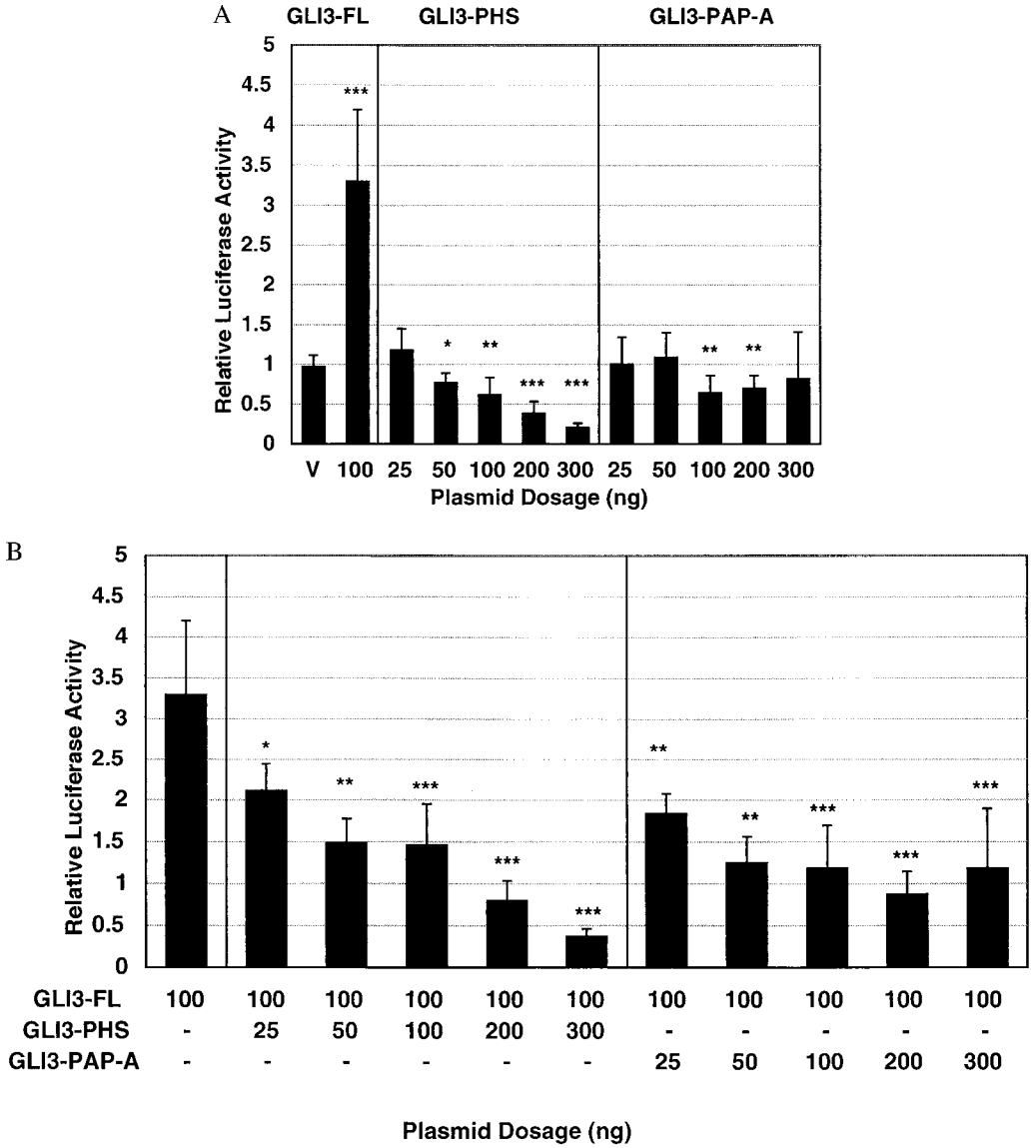

FIG. 3. Effects of mutant and full-length GLI3 constructs on the *PTCH1* reporter expression. (*A*) *GLI3* expression constructs were used to determine relative transcriptional activation or repression of *PTCH1* gene expression. *GLI3* constructs were cotransfected with a *PTCH1* reporter construct, allowing determination of *PTCH1* expression using the luciferase system. The GLI3-FL construct showed activation of *PTCH1* expression that was similar to that of unprocessed Ci^{155}. The GLI3-PHS construct showed dose-dependent repression of basal *PTCH1* activity, which was consistent with the lack of a transactivation domain and the presence of a zinc finger DNA-binding domain reminiscent of the effect of Ci^{75}. The GLI3-PAP-A construct did not consistently lower the basal level of *PTCH1* expression. Asterisks denote statistical significance in level compared with vector alone; *, $P < 0.02$; **, $P < 0.005$; ***, $P < 0.0001$ by Student's *t* test or Mann–Whitney *U* test (see *Materials and Methods*). V, vector alone at 100 ng. (*B*) The GLI3-PHS construct caused a dose-dependent repression of GLI3-FL-induced *PTCH1* promoter activity consistent with its lack of a transactivation domain and constitutive nuclear localization. In comparison, the GLI3-PAP-A construct (which was associated with a mixed cytoplasmic and nuclear localization; see Fig. 2*D*) did not cause a dose-dependent reduction in GLI3-FL-induced *PTCH1* expression levels, although the levels are all significantly lower than the GLI3-FL-induced *PTCH1* expression. Asterisks denote statistical significance in level compared with transfection of GLI3-FL (100 ng) alone; *, $P < 0.01$; **, $P < 0.001$; ***, $P < 0.0001$ by Student's *t* test or Mann–Whitney *U* test (see *Materials and Methods*).

consistent with our hypothesis of a dual function (activator and repressor) for this protein (4). Furthermore, this observation suggests that GLI3 could activate downstream genes in response to sonic hedgehog (Shh) signaling. Previous studies have failed to show activation of either HNF3β promoter (hepatocyte nuclear factor 3 beta) constructs (16) or multimerized consensus GLI-binding sites by GLI3 (17, 18), leading to suggestions that GLI3 is a monofunctional transcriptional repressor. A possible explanation for the different findings is that GLI3 may cooperate with some other factor(s) for a transactivation effect and thereby possesses a distinct target-gene specificity compared with GLI1 (19). The experiments in the present report used the natural *PTCH1* promoter in contrast to synthetic multimers of GLI consensus-binding sites used in previous studies. Although the absolute values of the transcriptional repression and activation in our experiments are smaller than those obtained by using synthetic promoters, they are statistically significant and are more likely to reflect true biologic effects of GLI3 than are studies that rely on synthetic promoters.

The data obtained in the present study support a model in which GLI3 mimics the bifunctional nature of the *Drosophila* Ci protein. The ability of mutant GLI3 proteins to repress downstream target genes in contrast to the activating effect of full-length GLI3 is consistent with the distinct developmental anomalies that are caused by these mutant proteins. It has been

demonstrated that in Xt^J, a mouse model for GCPS, reduced *GLI3* expression leads to ectopic activation of Shh in the anterior limb bud (20), which may be mediated through the relief of repression of HNF3β (16, 21), and results in preaxial digit duplication. According to our model, in PHS and PAP-A, the expression of mutant protein would be expected to result in repression of target genes. This, in turn, may have effects on postaxial digit formation, possibly by modulating Hoxd-12 expression, which promotes the formation of posterior chondrogenic condensations (22). It will be interesting to learn whether the observed subcellular localization and transcriptional effects of mutant GLI3 proteins are an indication that GLI3 is processed physiologically to a truncated repressor in the sonic hedgehog pathway as a mechanism of posttranslational regulation or whether these mutations merely mimic the mechanism of processed and unprocessed Ci proteins. Further elucidation of the mechanism of GLI3 subcellular translocation, interaction with potential mammalian homologues of the *Drosophila fused, su(fu),* and *costal2* gene products, and the existence or absence of GLI3 proteolytic processing *in vivo* will shed light on these issues. In this way, clinical and molecular analyses of human malformations can be an effective tool to elucidate mechanisms of gene action in normal and aberrant embryonic development.

We thank Drs. M. Chamorro, K. Kinzler, R. Nussbaum, W. Pavan, M. Rosenberg, S. Suchy, P. Schwartzberg, B. Vogelstein, and T. Wynshaw-Boris for technical advice, critical review of previous versions of this manuscript, and provision of Gli3 cDNA clones. Financial support for P.K., E.L., and R.T. was obtained from the Swedish Cancer Fund, the Swedish Children's Cancer Fund, and the National Swedish Board for Radiation Protection.

1. Vortkamp, A., Gessler, M. & Grzeschik, K.-H. (1991) *Nature (London)* **352,** 539–540.
2. Kang, S., Graham, J. M., Jr., Olney, A. H. & Biesecker, L. G. (1997) *Nat. Genet.* **15,** 266–268.
3. Radhakrishna, U., Wild, A., Grzeschik, K.-H. & Antonarakis, S. E. (1997) *Nat. Genet.* **17,** 269–270.
4. Biesecker, L. G. (1997) *Nat. Genet.* **17,** 259–260.
5. Ruppert, J. M., Vogelstein, B., Arheden, K. & Kinzler, K. W. (1990) *Mol. Cell. Biol.* **10,** 5408–5415.
6. Aza-Blanc, P., Ramírez-Weber, F.-A., Laget, M.-P., Schwartz, C. & Kornberg, T. B. (1997) *Cell* **89,** 1043–1053.
7. Robbins, D. J., Nybakken, K. E., Kobayashi, R., Sisson, J. C., Bishop, J. M. & Thérond, P. P. (1997) *Cell* **90,** 225–234.
8. Monnier, V., Dussillol, F., Alves, G., Lamour-Isnard, C. & Plessis, A. (1998) *Curr. Biol.* **8,** 583–586.
9. Ruiz i Altaba, A. (1997) *Cell* **90,** 193–197.
10. Biesecker, L. G. & Graham, J. M., Jr. (1996) *J. Med. Genet.* **33,** 585–589.
11. Finnigan, D. P., Clarren, S. K. & Haas, J. E. (1991) *Am. J. Med. Genet.* **40,** 395–400.
12. Wild, A., Kalff-Suske, M., Vortkamp, A., Bornholdt, D., König, R. & Grzeschik, K.-H. (1997) *Hum. Mol. Genet.* **6,** 1979–1984.
13. Hahn, H., Wicking, C., Zaphiropoulous, P. G., Gailani, M. R., Shanley, S., Chidambaram, A., Vorechovsky, I., Holmberg, E., Unden, A. B., Gillies, S., *et al.* (1996) *Cell* **85,** 841–851.
14. Lee, J., Platt, K. A., Censullo, P. & Ruiz i Altaba, A. (1997) *Development* **124,** 2537–2552.
15. Buscher, D., Bosse, B., Heymer, J. & Rüther, U. (1997) *Mech. Dev.* **62,** 175–182.
16. Sasaki, H., Hui, C., Nakafuku, M. & Kondoh, H. (1997) *Development* **124,** 1313–1322.
17. Vortkamp, A., Gessler, M. & Grzeschik, K. H. (1995) *DNA Cell Biol.* **14,** 629–634.
18. Yoon, J. W., Liu, C. Z., Yang, J. T., Swart, R., Iannaccone, P. & Walterhouse, D. (1998) *J. Biol. Chem.* **273,** 3496–3501.
19. Liu, F., Massagué, J. & Ruiz i Altaba, A. (1998) *Nat. Genet.* **20,** 325–326.
20. Masuya, H., Sagai, T., Moriwaki, K. & Shiroishi, T. (1997) *Dev. Biol.* **182,** 42–51.
21. Chang, B. E., Blader, P., Fischer, N., Ingham, P. W. & Strahle, U. (1997) *EMBO J.* **16,** 3955–3964.
22. Knezevic, V., De Santo, R., Schughart, K., Huffstadt, U., Chiang, C., Mahon, K. & Mackem, S. (1997) *Development* **124,** 4523–4536.